Influence of Alkalis and Sulphates on the Mineralogical Composition of Clinker

E. Gotti[1], M. Marchi[1], and U. Costa[1]
[1] *CTG – Italcementi Group, Bergamo, Italy*

1 Introduction

The presence of minor constituents such as MgO, K_2O, Na_2O or SO_3 in the raw materials or in the fuels affects the clinkering process both thermodynamically, by modifying the phase stability volumes in the quaternary system $CaO\text{-}SiO_2\text{-}Al_2O_3\text{-}Fe_2O_3$ [1], and kinetically, by modifying the chemical and physical properties of the interstitial melt that exert a great influence on the crystal growth [2].
A recent study on the influence of SO_3 on the phase relationship in the quaternary system has shown that an increase in the SO_3 content causes a reduction of the primary phase volume of C_3S and a change in the peritectic reaction occurring at the invariant point involving C_3S, C_2S, C_3A, C_4AF and liquid [3].
In a previous study [4] conducted on a rather large number of industrial clinkers, the quantitative phase analysis by means of X-Ray Diffraction and Rietveld Method (hereafter RQPA) had confirmed a strong influence of SO_3 and alkali contents on the mineralogical composition of clinker and consequently on the physical-mechanical properties of the resulting cements.
The present work reports about a further investigation into the influence of SO_3 and Na_2O on the equilibrium phase composition of sintered mixes of pure components having the typical chemical modules of an industrial clinker.

2 Sample preparation

Six basic mixes of pure $CaCO_3$, SiO_2, Al_2O_3 and Fe_2O_3, were prepared in order to obtain bulk compositions having lime saturation factor (LSF) from 0.92 to 0.98, alumina ratio (AR) from 1.15 to 2.00 and silica ratio (SR) equal to 2.50.
The range of AR values was chosen according to the quaternary phase diagram and so that they correspond to those points having an initial liquid composition above, at and below the invariant point [5].

SO_3-bearing samples were prepared by using pure $CaSO_4 \cdot 2H_2O$ as supplementary raw material in order to have 0.75, 1.50 and 2.50 wt% of SO_3 in the sintered material.
For Na_2O-bearing samples, pure Na_2CO_3 was added to the six basic mixes, in order to have 0.75, 1.00 and 1.50 wt% of Na_2O respectively in the sintered material.
The chemical compositions of all raw mixes were checked by means of X-ray fluorescence analyses.
Particular care was devoted to preparing the samples to guarantee not only the foreseen chemical compositions, but also good homogeneity.
For this reason, all the raw materials were ground to fineness lower than 40 μm and mixing was performed in cyclohexane.
The dried powders were also pre-calcined at 950°C in order to obtain CO_2-free samples.

3 Experimental

Raw mixes were pressed into pellets to increase the contact surface between the different components.
After crushing, pellets were placed in small platinum tubes with an inner diameter of 5 mm.
For SO_3 and Na_2O-bearing samples, platinum tubes were cap-sealed by using an arc-sealer, to suppress SO_3 and Na_2O evaporation.
Burning was performed in a Deltech DT-31-VT vertical muffle by applying the following time-temperature profile: heating from 900 to 1500 °C at a rate of 6 °C/min, constant temperature of 1500°C for 90 min, cooling to 1300 °C at a rate of 4 °C/min, quenching to room temperature.
The phase diagram indicates that a certain amount of liquid phase coexists at equilibrium with C_3S and C_2S at 1500°C. The cooling rate applied from 1500 °C down to 1300°C was considered slow enough to achieve the chemical equilibrium during solidification.
All experiments were conducted in air; in this relatively oxidizing atmosphere, iron can be almost entirely considered as Fe^{3+} and virtually no loss of iron occurs by its reaction with the platinum tube.
X-Ray Powder Diffraction (XRD) and microscopy analyses were performed on the sintered materials to determine type, amount and chemical composition of the phases produced in the sintering process.
XRD patterns have been collected using a SIEMENS D-5000 diffractometer with instrumental Bragg-Brentano geometry, equipped with a Cu-tube (λ = 1.5456 Å) and a graphite monochromator on the diffracted beam.
The adopted experimental conditions were: tube power of 40KV, 40mA, fixed divergence and anti-scattering slits equal to 1°, receiving slit aperture of 0.1 mm, sample holder spinning of 30 rpm.

Diffraction patterns were collected from 10 to 70° 2θ, at a scanning step of 0.02° 2θ and counting time of 4 sec/step.
All the patterns were refined by means of the Rietveld method to obtain also quantitative information; these analyses were conducted using the TOPAS software [6].
Microstructure of the sintered materials was observed on polished sections under a Reflected Light Microscope (Reichert MeF3A) and a Scanning Electron Microscope (LEO 1450VP).
Moreover, the chemical composition of the mineralogical phases was determined by using an Energy Dispersive Spectrometer connected to the SEM (Gresham Sirius 10 detector and iXRF Iridium interface).

4 Results and discussion

Mineralogical compositions of the six basic clinkers obtained by RQPA and Bogue calculation are given in Table 1.

Table 1: RQPA and Bogue mineralogical composition of the six basic clinkers.

	C_3S (wt%)		C_2S (wt%)		C_3A (wt%)		C_4AF (wt%)	
sample	*RQPA*	*Bogue*	*RQPA*	*Bogue*	*RQPA*	*Bogue*	*RQPA*	*Bogue*
LSF 0.92, AR 1.15	*69.6*	*59.7*	*14.5*	*21.4*	*6.4*	*5.9*	*9.5*	*13.1*
LSF 0.92, AR 1.38	*59.5*	*58.2*	*24.4*	*22.4*	*7.6*	*7.6*	*8.5*	*11.8*
LSF 0.92, AR 2.00	*57.3*	*55.3*	*25.1*	*24.3*	*12.7*	*11.1*	*5.0*	*9.3*
LSF 0.98, AR 1.15	*80.7*	*74.4*	*4.4*	*7.5*	*5.6*	*5.6*	*9.3*	*12.5*
LSF 0.98, AR 1.38	*75.3*	*72.9*	*6.3*	*8.4*	*8.2*	*7.3*	*10.3*	*11.3*
LSF 0.98, AR 2.00	*74.8*	*70.2*	*6.6*	*10.2*	*13.2*	*10.6*	*5.3*	*8.9*

The content of the main constituents in the samples reflects the different chemical compositions of the starting mixes: the C_3S content increases with increasing LSF and decreasing AR, while C_3A content increases with increasing AR; trends of C_2S and C_4AF contents are opposite to those of C_3S and C_3A respectively.
Some deviations of RQPA composition compared to the theoretical Bogue values are most apparent.
The C_3S content is higher and the total content in aluminate phases (C_3A+C_4AF) is usually lower except for sample with LSF=0.98 and AR=1.38.
SEM-EDS analyses show that these differences are probably due to the inclusion of foreign elements in the lattice of clinker phases rather than non-equilibrium conditions during the experiments.
In fact, the lower total aluminate content is clearly due to the inclusion of Al and Fe in the silicate phases (see Fig. 1 and 2) that reduces their availability for aluminate and ferrite formation.
As a consequence, some of the lime not combined in the aluminate phases contributes to the formation of additional C_3S.

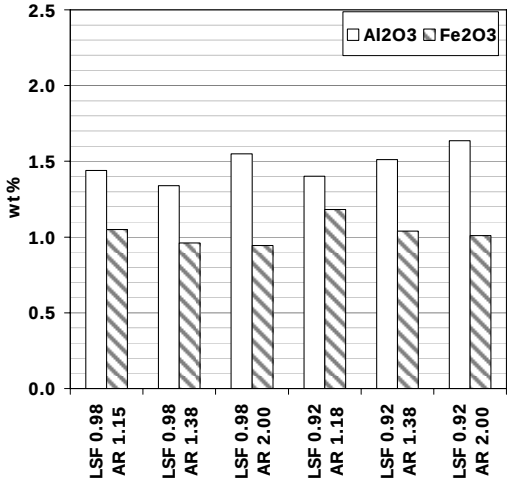

Fig. 1: Chemical composition of C_3S obtained by SEM-EDS analysis.

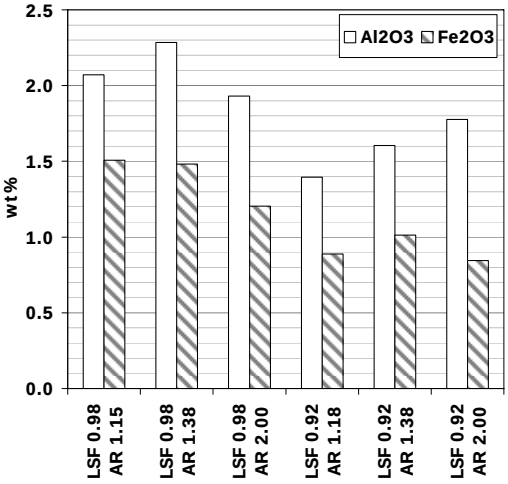

Fig. 2: Chemical composition of C_2S obtained by SEM-EDS analysis.

The microstructural characteristics of the sintered materials confirm the good homogeneity of the raw mixes, an adequate burning time and an appropriate cooling rate to achieve equilibrium conditions.
In all samples alite appears as idiomorphous crystals with dimensions of about 20 μm, while belite is homogeneously distributed showing rounded shape crystals with average dimensions of about 35 μm.
Smaller crystal sizes are observed in the samples with the highest LSF or the highest AR.
Interstitial phase appears coarsely crystallized and made only by cubic C_3A and C_4AF.
The sample porosity is generally low for all the clinkers.
These microstructural characteristics do not differ much from those of industrial clinkers.

4.1 Influence of SO_3

Eighteen SO_3-bearing raw mixes were sintered to evaluate the influence of SO_3 on the mineralogical composition of clinker.
Results of the RQPA are given in Table 2.
A small amount of residual $CaSO_4$ (anhydrite) was detected in the sintered materials containing 2.5 wt% of SO_3.
A change in the amount of C_3S and C_2S as a function of the SO_3 content is apparent.
The C_3S/C_2S wt. ratio is strongly reduced in SO_3-bearing samples respect to their correspondent SO_3-free samples (see Fig. 3).
In the samples containing 2.5 wt% of SO_3, C_3S is practically undetectable and a large amount of free lime is found.

These results are in good agreement with previous studies showing that the primary phase volume of C_3S tends to shrink with the increase of the SO_3 content and finally disappears [3].

Table 2: RQPA results for the clinkers containing different amounts of SO3. Results are expressed as wt%.

sample	*SO_3*	*C_3S*	*C_2S*	*C_3A*	*C_4AF*	*Free lime*	*$CaSO_4$*
	0.0	*69.6*	*14.5*	*6.4*	*9.5*	-	-
LSF 0.92	*0.75*	*53.1*	*31.4*	*5.5*	*10.0*	-	-
AR 1.15	*1.5*	*40.1*	*47.7*	*3.9*	*8.3*	-	-
	2.5	*4.4*	*72.5*	*4.1*	*11.2*	*7.7*	*0.2*
	0.0	*59.5*	*24.4*	*7.6*	*8.5*	-	-
LSF 0.92	*0.75*	*55.4*	*26.5*	*9.5*	*8.6*	-	-
AR 1.38	*1.5*	*51.4*	*33.9*	*5.5*	*9.1*	-	-
	2.5	*2.1*	*70.7*	*4.6*	*9.6*	*6.7*	*0.3*
	0.0	*57.3*	*25.1*	*12.7*	*5.0*	-	-
LSF 0.92	*0.75*	*49.0*	*34.9*	*11.3*	*4.8*	-	-
AR 2.00	*1.5*	*46.1*	*38.9*	*11.2*	*3.8*	-	-
	2.5	*0.0*	*72.2*	*11.8*	*8.3*	*6.6*	*0.6*
	0.0	*80.7*	*4.4*	*5.6*	*9.3*	-	-
LSF 0.98	*0.75*	*59.6*	*22.7*	*7.0*	*10.8*	-	-
AR 1.15	*1.5*	*60.1*	*23.9*	*5.9*	*10.1*	-	-
	2.5	*0.0*	*72.4*	*3.0*	*13.3*	*10.9*	*0.3*
	0.0	*75.3*	*6.3*	*8.2*	*10.3*	-	-
LSF 0.98	*0.75*	*60.8*	*22.4*	*8.3*	*8.5*	-	-
AR 1.38	*1.5*	*64.0*	*21.1*	*6.9*	*8.0*	-	-
	2.5	*0.0*	*71.5*	*4.5*	*13.5*	*10.3*	*0.2*
	0.0	*74.8*	*6.6*	*13.2*	*5.3*	-	-
LSF 0.98	*0.75*	*50.2*	*30.7*	*14.0*	*5.0*	-	-
AR 2.00	*1.5*	*60.9*	*22.4*	*9.4*	*7.4*	-	-
	2.5	*0.0*	*69.3*	*7.7*	*12.4*	*10.4*	*0.2*

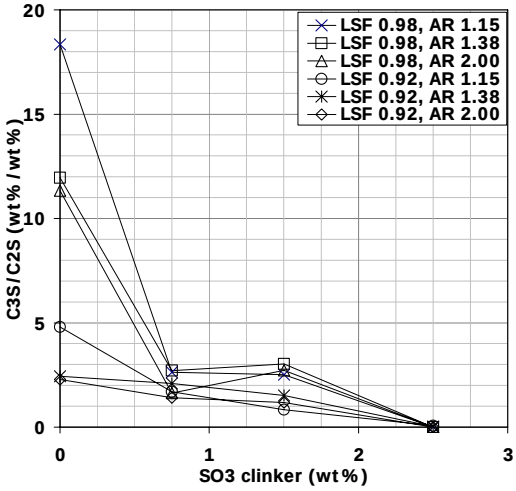

Fig. 3: C_3S/C_2S wt. ratio as a function of SO_3 content in the clinkers

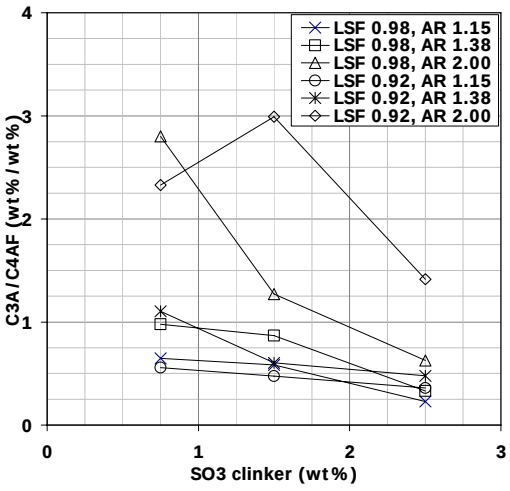

Fig. 4: C_3A/C_4AF wt. ratio as a function of SO_3 content in the clinkers

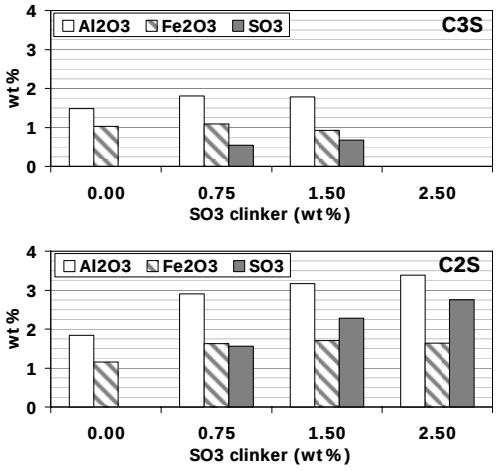

Fig. 5: Al_2O_3, Fe_2O_3 and SO_3 contents in C_3S and C_2S as obtained by SEM-EDS analysis of the clinkers containing different amounts of SO_3

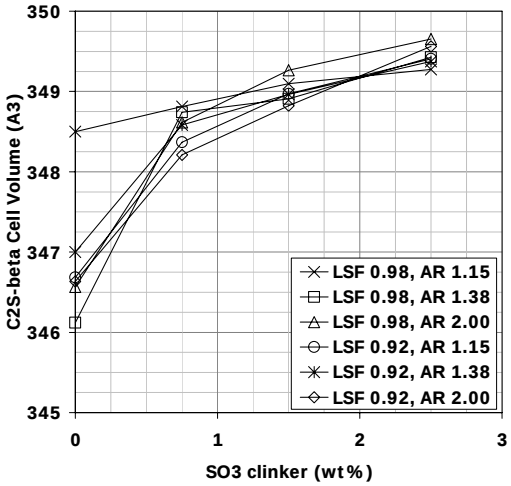

Fig. 6: β-C_2S cell volume variation as a function of SO_3 content in the clinkers

The C_3A content decreases with increasing SO_3 contents in all samples.
The C_4AF content remains constant or slightly increases for SO_3 content up to 1.5 wt%.
In the samples with 2.5 wt% of SO_3, the C_4AF content considerably increases, since a peritectic reaction $L+C_2S \rightarrow CaO+C_4AF$ occurs [3].
As a consequence the C_3A/C_4AF wt. ratio is shifted to smaller values, with one exception (Fig. 4).
The chemical composition obtained by SEM-EDS shows that sulphur is exclusively incorporated in the silicate phases and preferentially in C_2S, confirming other previous observations [7].
Both Al and Fe are incorporated in larger amounts in C_2S than in C_3S (see Fig. 5).
The Al and Fe content in silicate phases rises by the increase of SO_3 and this effect is especially apparent for Al.
The higher amount of inclusions in the silicates structure is also supported by the increase in the C_2S cell volume, as detected by XRD for the sample containing SO_3 (see Fig. 6).
According XRD patterns [8], C_3S seems to be exclusively present as M1 polymorph and its crystal size is also increased by the presence of SO_3 for the well-known mineralizing effect due to sulfate (see Fig. 7) [9, 10].

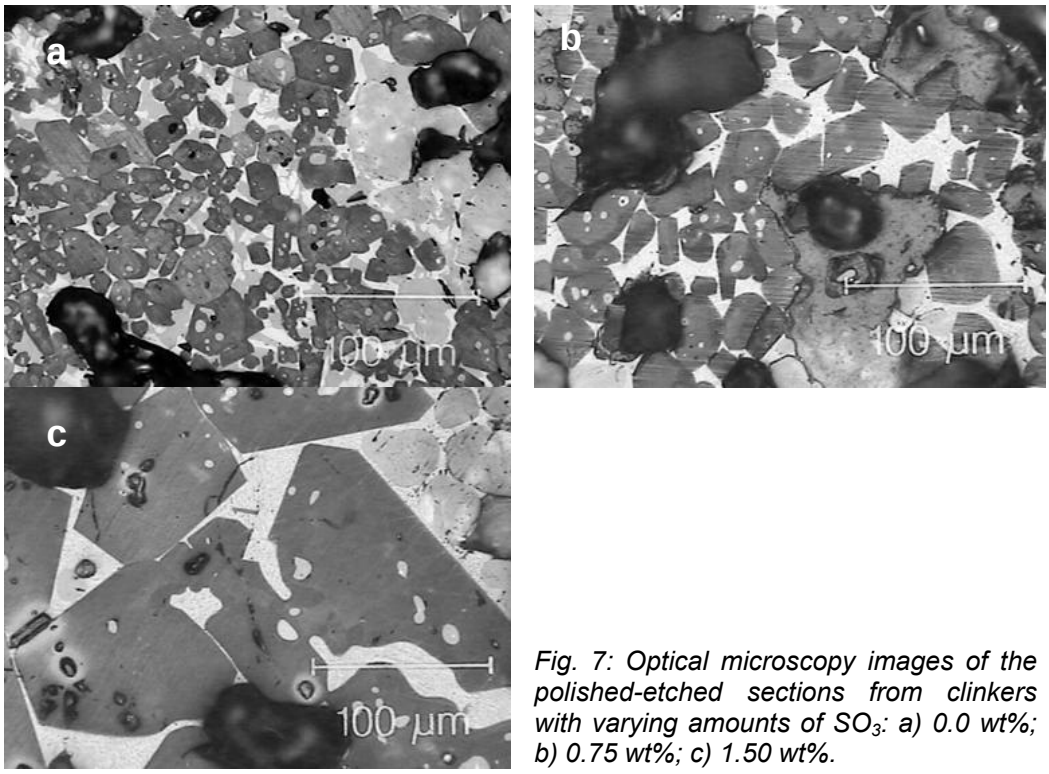

Fig. 7: Optical microscopy images of the polished-etched sections from clinkers with varying amounts of SO_3: a) 0.0 wt%; b) 0.75 wt%; c) 1.50 wt%.

4.2 Influence of Na_2O

Eighteen Na_2O-bearing raw mixes were sintered to evaluate the influence of Na_2O on the mineralogical composition of clinker.
Results of the RQPA are given in Table 3.
The addition of Na_2O to the mixes leads to a strong modification of the mineralogical composition of the clinkers as detected by XRD and optical microscopy (see Fig. 8 and 9).
In fact, in presence of Na_2O, orthorhombic C_3A appears and for Na_2O contents higher than 1.0 wt% it is the only polymorph present.
The total C_3A content increases by 4 wt% in clinkers containing Na_2O, while the C_4AF content decreases by 2 wt%.
Na_2O in the samples causes also the stabilization of high temperature polymorphs of C_2S.
In samples with 0.75 and 1.0 wt% of Na_2O beside the β form also the α' and α forms are present and their content tends to increase with increasing Na_2O.
Optical microscopy observations highlight a modification of the lamellar structure of belite crystals.
At increasing Na_2O contents, the frequency of striations is lower and they become coarser.
Striations in belite arise upon cooling through a α–to-α' transition and they split in two when the transition from α'_L to β occurs.

These microstructural characteristics confirm that the increase of Na_2O content causes the stabilization of high temperature polymorphs of belite.
SEM-EDS analyses show that the larger portion of Na is incorporated in the aluminate phases, mainly in C_3A, and only to a lesser extent in the silicate phases, with higher values found in C_2S than in C_3S.
Its replacement for Ca increases in all phases as the Na_2O content of the clinkers increases, reaching a maximum value of about 4 wt% in C_3A.
This substitution leaves additional lime available for the supplementary formation of C_3A and C_3S, as shown by XRD analyses.
The SEM-EDS analysis reveals that in presence of Na_2O, C_3S has a lower CaO/SiO_2 wt. ratio and the aluminate phases have a SiO_2 content that is almost twice as great.
In samples with LSF=0.98, a certain amount of free lime is detected for high Na_2O contents, while this does not occur in the same samples Na_2O-free or in samples with LSF=0.92 (see Table 3).
Based on these observations, it can be supposed that the upper limit of the lime saturation factor to prevent primary crystallization of free lime is reduced.
This could be justified by the primary stability volume of C_3S moving away from the CaO corner in the quaternary diagram.

Table 3: RQPA results for the clinkers containing different amount of Na_2O. Results are expressed as wt%.

sample	*Na_2O*	*C_3S*	*β-C_2S*	*α'-C_2S*	*α-C_2S*	*C_2S_{TOT}*	*C_3A_{cub}*	*C_3A_{ortho}*	*C_3A_{TOT}*	*C_4AF*	*Free lime*
	0.0	*69.6*	*14.5*	*-*	*-*	*14.5*	*6.4*	*-*	*6.4*	*9.5*	*-*
LSF 0.92	*0.75*	*69.5*	*-*	*11.5*	*1.6*	*13.2*	*-*	*10.0*	*10.0*	*7.4*	*-*
AR 1.15	*1.0*	*69.6*	*-*	*9.2*	*3.6*	*12.8*	*-*	*10.8*	*10.8*	*6.8*	*-*
	1.5	*75.0*	*-*	*-*	*5.5*	*5.5*	*-*	*14.3*	*14.3*	*5.2*	*-*
	0.0	*59.5*	*24.4*	*-*	*-*	*24.4*	*7.6*	*-*	*7.6*	*8.5*	*-*
LSF 0.92	*0.75*	*60.4*	*5.4*	*14.1*	*3.4*	*22.9*	*4.7*	*5.8*	*10.5*	*6.2*	*-*
AR 1.38	*1.0*	*62.3*	*-*	*14.7*	*4.7*	*19.4*	*-*	*12.9*	*12.9*	*5.4*	*-*
	1.5	*70.5*	*-*	*2.5*	*7.6*	*10.0*	*-*	*14.9*	*14.9*	*4.5*	*-*
	0.0	*57.3*	*25.1*	*-*	*-*	*25.1*	*12.7*	*-*	*12.7*	*5.0*	*-*
LSF 0.92	*0.75*	*57.4*	*8.2*	*12.3*	*2.5*	*23.0*	*4.6*	*11.4*	*16.0*	*3.7*	*-*
AR 2.00	*1.0*	*62.1*	*-*	*14.1*	*3.3*	*17.4*	*-*	*17.0*	*17.0*	*3.5*	*-*
	1.5	*67.1*	*-*	*8.0*	*6.5*	*14.5*	*-*	*15.1*	*15.1*	*3.3*	*-*
	0.0	*80.7*	*4.4*	*-*	*-*	*4.4*	*5.6*	*-*	*5.6*	*9.3*	*-*
LSF 0.98	*0.75*	*77.6*	*0.4*	*4.5*	*0.0*	*5.0*	*-*	*12.3*	*12.3*	*5.2*	*-*
AR 1.15	*1.0*	*80.2*	*-*	*0.0*	*2.7*	*2.7*	*-*	*11.9*	*11.9*	*5.2*	*-*
	1.5	*80.5*	*-*	*0.0*	*0.9*	*0.9*	*-*	*13.2*	*13.2*	*5.3*	*-*
	0.0	*75.3*	*6.3*	*-*	*-*	*6.3*	*8.2*	*-*	*8.2*	*10.3*	*-*
LSF 0.98	*0.75*	*78.4*	*-*	*1.8*	*1.7*	*3.5*	*-*	*12.6*	*12.6*	*5.6*	*-*
AR 1.38	*1.0*	*79.9*	*-*	*0.2*	*2.3*	*2.5*	*-*	*11.6*	*11.6*	*5.4*	*0.6*
	1.5	*78.7*	*-*	*0.0*	*0.9*	*0.9*	*-*	*16.0*	*16.0*	*3.2*	*1.3*
	0.0	*74.8*	*6.6*	*-*	*-*	*6.6*	*13.2*	*-*	*13.2*	*5.3*	*-*
LSF 0.98	*0.75*	*74.9*	*1.5*	*3.4*	*1.8*	*6.7*	*-*	*14.4*	*14.4*	*4.0*	*-*
AR 2.00	*1.0*	*75.7*	*-*	*2.6*	*1.8*	*4.6*	*-*	*16.4*	*16.4*	*3.2*	*-*
	1.5	*79.4*	*-*	*1.5*	*1.9*	*3.4*	*-*	*13.7*	*13.7*	*2.8*	*0.6*

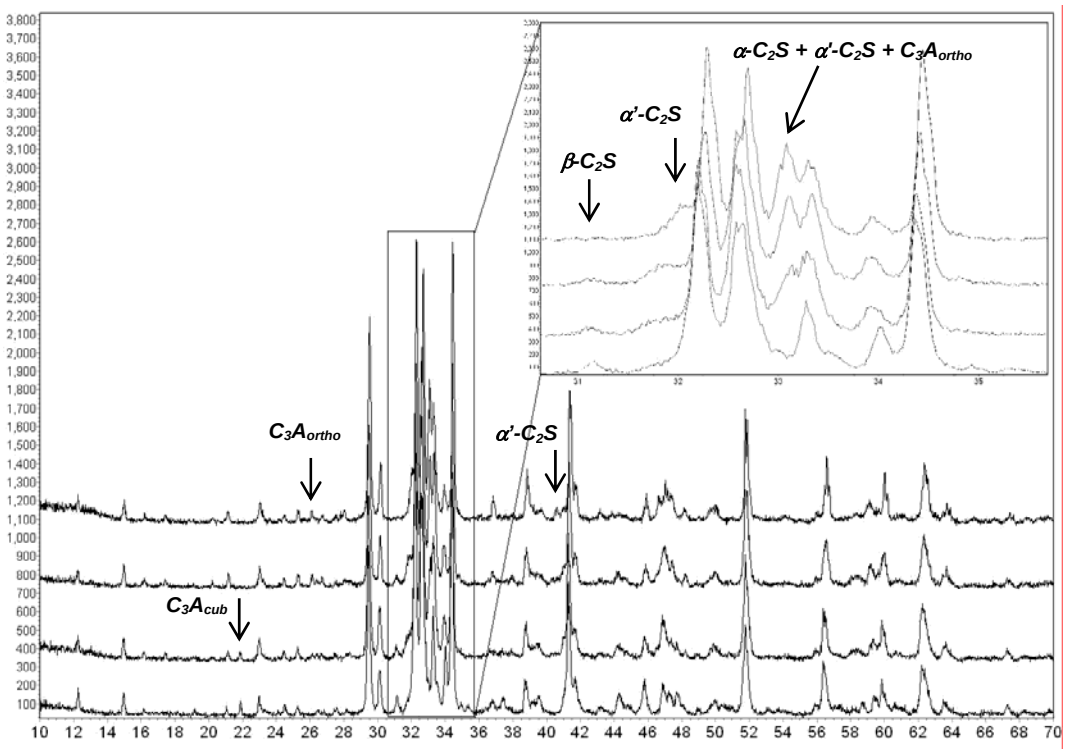

Fig. 8: X-ray patterns of the clinkers with different Na_2O contents. C_3A_{cub} peak at 21.9°2θ disappears for Na_2O contents >0.5 wt% while C_3A_{ortho} peak at 26.1 °2θ becomes detectable. The intensity of β-C_2S peaks at 31.2 and 37.5 °2θ decreases with increasing Na_2O contents and the peaks of α'-C_2S at 40.5 °2θ and α-C_2S at 32°2θ appear.

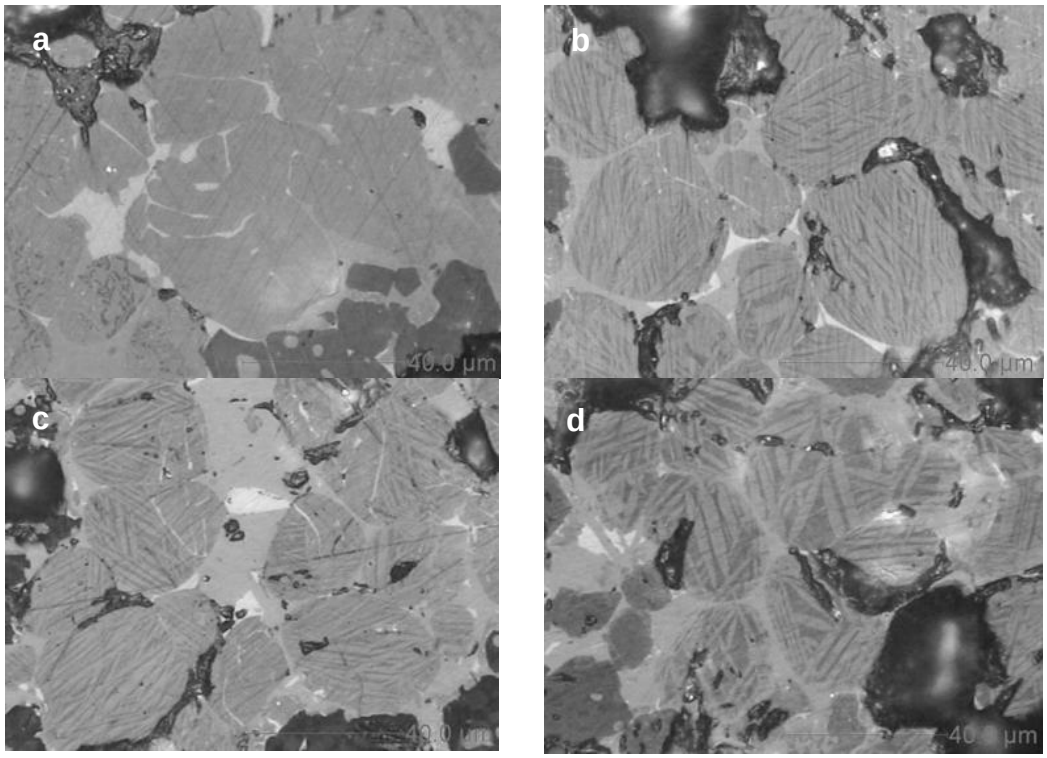

Fig. 9: Optical microscopy images of the polished-etched sections from clinkers with varying amounts of Na_2O: a) 0.0 wt%; b) 0.75 wt%; c) 1.0 wt%; d) 1.5 wt%.

SEM-EDS analyses show that the iron content in C_3A increases from 5-6 wt% in the clinker having the lowest Na_2O content to 9-15 wt% in the clinkers with the highest Na_2O contents.
Moreover, the increase of C_3A/C_4AF wt. ratio (Table 3) suggests that the presence of Na_2O causes a decrease of the Al_2O_3/Fe_2O_3 ratio of the invariant point.
XRD pattern inspection shows that C_3S is exclusively in the M3 form [7] and its crystal size is also increased by the presence of Na_2O.

5 Conclusions

As the SO_3 content in the sintered materials increases, the C_3S primary phase volume is reduced in the quaternary phase diagram, resulting in a decrease of C_3S/C_2S wt. ratio.
For the samples considered, 2.5 wt. % is the limit of SO_3 content at which C_3S is not formed.
Sulphur is preferentially incorporated in the silicate phases (mainly C_2S) and the inclusions of Al and Fe increase as SO_3 increases.
For this reason, the aluminates content decreases with increasing SO_3 content, such as the C_3A/C_4AF ratio.
The C_4AF content considerably increases only in those samples with 2.5 wt% content of SO_3, due to the occurrence at the invariant point of the peritectic reaction $L+C_2S \rightarrow CaO+C_4AF$.
The addition of Na_2O to the mixes strongly modifies the mineralogical composition of the sintered materials: orthorhombic C_3A appears and becomes the only C_3A polymorph present when the Na_2O content is higher than 1.0 wt%.
Na is mainly incorporated in C_3A and its content limit is 4 wt% (expressed as Na_2O). Na is partly incorporated in C_2S, causing the stabilization at room temperature of the forms α and α'.
The increase of the Na_2O content in the clinkers leads to a C_2S content decrease and a C_3S content increase.
For high amounts of Na_2O, the appearance of the equilibrium free lime in the clinkers with an LSF of 0.98 is observed.
This can be explained by a reduction of the maximum acceptable CaO content of the mixes with Na_2O that derives from the fact that the C_3S primary stability volume moves away from the CaO corner in the quaternary system.
At the same time, the decrease in the Al_2O_3 to Fe_2O_3 ratio of the invariant point causes an increase of the C_3A/C_4AF wt. ratio.
These results justify previous observations concerning the effects of SO_3 and Na_2O on the mineralogical composition of industrial clinker [4].

References

[1] Lea's, Chemistry of Cement and Concrete, 4rd ed., Edward Arnold Ltd., England, 1998

[2] V.V. Timashev, The Kinetic of Clinker Formation. The Structure and Composition of Clinker and its Phases, Proceedings of the 7th ICCC, Paris, 1, (I-3), (1980), 1-17

[3] S. Uda, E. Asakura and M. Nagashima, Influence of SO_3 on the Phase Relationship in the System CaO-SiO_2-Al_2O_3-Fe_2O_3, J. Am. Ceram. Soc., 81(3) (1998) 725-729

[4] U. Costa and M. Marchi, Mineralogical Composition of Clinker by Bogue and Rietveld Method: The Effect of Minor Elements, Proceedings of the 11th ICCC (2003) 151-159

[5] F.M. Lea and T.W. Parker, The Quaternary System CaO-Al_2O_3-SiO_2-Fe_2O_3 in Relation to Cement Technology, Building Research Technical Paper, 16, London: H.M.S.O. (1935), 52 pp

[6] Bruker AXS, TOPAS V2.1: General Profile and Structure Analysis Software for Powder Diffraction Data, User Manual, Bruker AXS, (2003), Karlsruhe, Germany

[7] H.F.W. Taylor, Distribution of Sulphate between Phases in Portland Cement Clinkers, Cem. Concr. Res., 29, (1989), 1173-1179

[8] M. Courtial, M.-N. de Noirfontaine, F. Dunstetter, G. Gasecki and M. Signes-Frehel, Polymorphism of Tricalcium Silicate in Portland Cement: A Fast Visual Identification of Structure and Superstructure, Powder Diffraction, 18 (1), (2003), 7-15

[9] I. Maki, Relationship of Processing Parameters to Clinker Properties: Influence of Minor Components, Proceedings of the 8th ICCC, Rio de Janeiro, (1), (1986), 34-47

[10] I. Maki and K. Goto, Factors Influencing the Phase Constitution of Alite in Portland Cement Clinker, Cem. Concr. Res., 12(3), (1982), 301-308